AD-A181 206 EVALUATION OF A DIFFUSION/TRAPPING MODEL FOR HYDROGEN INGRESS IN HIGH-STRENGTH ALLOYS(U) SRI INTERNATIONAL MENLO PARK CA B G POUND 14 MAY 87 N00014-86-C-0233 1/1

UNCLASSIFIED F/G 11/6 NL

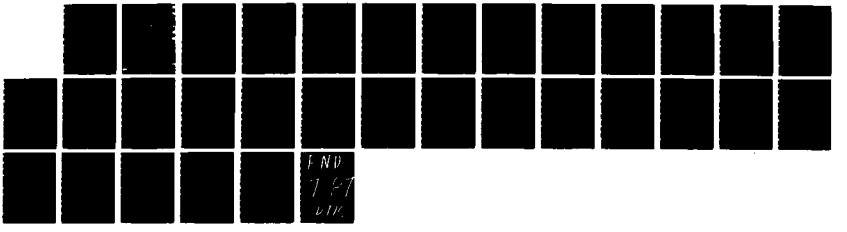

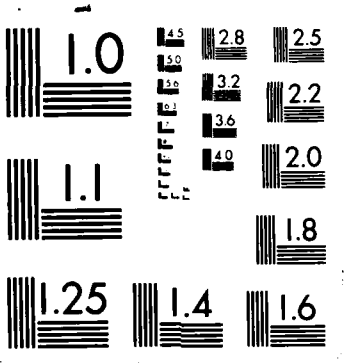
1.0
1.1
1.25
1.4
1.6
1.8
2.0
2.2
2.5
2.8
3.2
3.6
4.0
4.5
5.0
5.6
6.3

(12)

EVALUATION OF A DIFFUSION/TRAPPING MODEL FOR HYDROGEN INGRESS IN HIGH-STRENGTH ALLOYS

May 1987

Annual Report

By: Bruce G. Pound
Materials Research Laboratory

Prepared for:

DEPARTMENT OF THE NAVY
Office of Naval Research
800 N. Quincy Street
Arlington, VA 22217

Attention: Dr. A. J. Sedriks

Contract No. N00014-86-C-0233

SRI Project PYU-1962

SRI International
333 Ravenswood Avenue
Menlo Park, California 94025-3493
(415) 326-6200
TWX: 910-373-2046
Telex: 334486

REPORT DOCUMENTATION PAGE

1a REPORT SECURITY CLASSIFICATION: Unclassified	1b RESTRICTIVE MARKINGS
2a SECURITY CLASSIFICATION AUTHORITY	3 DISTRIBUTION/AVAILABILITY OF REPORT: Approved for public release-distribution unlimited. Reproduction in whole or part is permitted for any purpose of the U.S. Gov't.
2b DECLASSIFICATION/DOWNGRADING SCHEDULE	
4 PERFORMING ORGANIZATION REPORT NUMBER(S)	5 MONITORING ORGANIZATION REPORT NUMBER(S)
6a NAME OF PERFORMING ORGANIZATION: SRI International; 6b OFFICE SYMBOL (If applicable)	7a NAME OF MONITORING ORGANIZATION
6c ADDRESS (City, State, and ZIP Code): 333 Ravenswood Avenue, Menlo Park, CA 94025	7b ADDRESS (City, State, and ZIP Code)
8a NAME OF FUNDING/SPONSORING ORGANIZATION: Office of Naval Research; 8b OFFICE SYMBOL (If applicable)	9 PROCUREMENT INSTRUMENT IDENTIFICATION NUMBER: N00014-86-C-0233
8c ADDRESS (City, State, and ZIP Code): Metallic Materials, Code 1131M, 800 North Quincy Street, Arlington, VA 22217-5000	10 SOURCE OF FUNDING NUMBERS: PROGRAM ELEMENT NO. / PROJECT NO / TASK NO / WORK UNIT ACCESSION NO

11 TITLE (Include Security Classification)
Evaluation of a Diffusion/Trapping Model for Hydrogen Ingress in High-Strength Alloys (Unclassified)

12 PERSONAL AUTHOR(S)
B. G. Pound

13a TYPE OF REPORT	13b TIME COVERED	14 DATE OF REPORT (Year Month Day)	15 PAGE COUNT
Annual-Technical	FROM 86Mar15 TO 87Mar15	87 May 14	29

16 SUPPLEMENTARY NOTATION

17 COSATI CODES		
FIELD	GROUP	SUB-GROUP

18 SUBJECT TERMS (Continue on reverse if necessary and identify by block number)
4340 Steel, Monel K500, MP35N, hydrogen, ingress, models, hydrogen diffusion, hydrogen trapping, high-strength, alloys, hydrogen embrittlement.

19 ABSTRACT (Continue on reverse if necessary and identify by block number)

This report covers work performed during the first year of a program to apply a diffusion/trapping model for hydrogen ingress in three high-strength alloys, AISI 4340 steel, Monel K500, and MP35N. The model is coupled to the use of a potentiostatic double-pulse technique, and current transient data were obtained for the alloys in 1 M HAc/1 M NaAc (Ac = acetate) with 15 ppm As_2O_3. In all cases, the anodic charge can be analyzed as a function of charging time in terms of an interfacial control model in which the rate of H ingress into the metal is determined by the flux across the metal surface.

The 4340 steel was tested at yield strengths of approximately 175 and 250 ksi The rate constant for irreversible trapping, k, was evaluated from the measured or apparent rate constant, k_a, by estimating the effect of reversible traps from diffusivity data and was found to be $4/s^{-1}$ for both 4340 specimens. Based on a simple model of spherical traps, k was used to determine the density of irreversible traps as $2 \times 10^8\ m^{-3}$. This value is in reasonable agreement with the number of MnS inclusions,

20 DISTRIBUTION/AVAILABILITY OF ABSTRACT	21 ABSTRACT SECURITY CLASSIFICATION
☒ UNCLASSIFIED/UNLIMITED ☐ SAME AS RPT ☐ DTIC USERS	Unclassified
22a NAME OF RESPONSIBLE INDIVIDUAL	22b TELEPHONE (Include Area Code) / 22c OFFICE SYMBOL

DD FORM 1473, 84 MAR — 83 APR edition may be used until exhausted. All other editions are obsolete.

continued from Block 19

2×10^9 m^{-3}, but is orders of magnitude less than the number of other possible irreversible traps such as Fe_3C and TiC interfaces.

The Monel K500 was tested at yield strengths of about 110 and 159 ksi. The apparent trapping constant decreased from 0.027 to 0.016 s^{-1} with the increase in yield strength. Because of a lack of diffusivity data, it was assumed that the reversible traps have little effect on the low diffusivity of H in Cu/Ni alloys and therefore, by implication, little effect on k. Accordingly, the values of k_a were used to evaluate the density of irreversible traps. The densities of 1.7×10^{21} and 9.9×10^{20} m^{-3} were a few orders of magnitude less than the number of S impurities, 1.6×10^{24} atoms m^{-3}, which were assumed to be the primary irreversible traps. This difference is thought to be largely attributable to assumptions regarding the H diffusivity in the Monel and neglecting the effect of reversible traps on k.

The apparent trapping constant for MP35N (yield strength = 269 ksi) was also measured, and using similar arguments to those for the Monel, the value of k was approximated to k_a, 0.025 s^{-1}. The resulting irreversible trap density of 8×10^{21} m^{-3} is three orders of magnitude less than the total content of S and P, 8.1×10^{24} atoms m^{-3}, which have been associated with hydrogen embrittlement in MP35N. Again, the numbers can largely be reconciled on the basis of assumptions for the H diffusivity in MP35N and the effect of reversible traps.

CONTENTS

TABLES

FIGURES

INTRODUCTION

The use of metals and alloys in aqueous environments is often limited by their susceptibility to hydrogen embrittlement. The ingress of hydrogen into steel and other alloys undergoing corrosion can severely affect the properties of these metals, especially where high-strength steels are used. In contrast, certain high-strength nickel-based alloys, such as Monel K500 and MP35N, appear to be considerably more resistant to hydrogen embrittlement.

Structural inhomogeneities such as dislocations, internal interfaces, and grain boundaries are potential trapping sites for the diffusing hydrogen. The hydrogen atoms are partioned between the traps and normal lattice sites depending on the binding energy of the hydrogen atom to the trapping site, and it is usual to classify traps as being reversible and irreversible.

A model was developed previously[1] to represent the diffusion and trapping of H atoms. The model is coupled to the use of a potentiostatic double-pulse technique that has been applied[2] to iron in H_2S solutions and was demonstrated to provide quantitative information on both the mobile and trapped hydrogen in the metal. The technique is a transient type rather than one involving steady-state measurements, as is more commonly used for electrochemical studies of hydrogen ingress. Indeed, the use of this technique has been reported only by one other group,[3] and H trapping was not considered in the data analysis.

The objective of this program is to apply this technique and associated model to a high-strength steel (AISI 4340) and two high-strength nickel-based alloys, MP35N and Monel K500. By analyzing the data in terms of this model for each metal, it is intended to provide some insight into the hydrogen ingress and trapping characteristics in relation to the differing resistance of these alloys to hydrogen embrittlement. The results obtained during the first year of the current program are presented in this report.

BACKGROUND

Previous electrochemical investigations of hydrogen ingress have been concerned mainly with H diffusion through thin metal membranes using controlled potential or current conditions at both interfaces. In contrast, the potentiostatic double-pulse (PDP) technique is applied to sections of bulk metal, typically but not necessarily in rod form. The metal is charged with hydrogen at a constant potential E_c for a time t_c usually in the range 0.5-40 s. The potential is then stepped to a more positive value, E_A (5-10 mV negative of the open-circuit potential), resulting in an anodic current transient involving a charge q_a due to reoxidation of H atoms at the same surface according to the reaction

$$H_{metal} \text{ ---> } H_{ads} \text{ ---> } H^+ + e^- \qquad (1)$$

where H_{ads} represents hydrogen atoms adsorbed at the metal surface.

The effect of trapping on the diffusion of hydrogen is taken into account by modifying Fick's Second Law of diffusion. The approach is to include a trapping term, kc, in which the rate of trapping is assumed to be proportional to the concentration, c(x,t), of diffusing H at point x:

$$dc/dt = D(d^2c/dx^2) - kc \qquad (2)$$

The magnitude of the trapping rate constant, k, is determined by the density of traps and the probability of capture of a hydrogen atom by a trap. In the simplest case, it is assumed that the trapping is entirely irreversible, so there is no significant release of H atoms from the traps. However, the model has been extended to allow for the effect of reversible traps on k according to the following relationship:

$$k_a = k/(1 + K_r) \qquad (3)$$

where K_r is the equilibrium constant for reversible traps, k is the irreversible trapping rate constant, and k_a is the apparent trapping constant measured for irreversible traps in the presence of reversible traps. The equilibrium constant is defined by $(k_r/p)N$ where k_r and p are the trapping and release rate constants for reversible traps and N is the density of reversible traps. This constant also relates the apparent diffusivity, D_a, to the lattice diffusivity, D_L, for hydrogen[4]:

$$D_a = D_L/(1 + K_r) \tag{4}$$

The value of K_r can therefore be determined from diffusivity data if known for the alloy of interest and also for the lattice of the primary component(s) of the alloy.

It is considered that the irreversible traps do not become saturated; that is, k is constant. This assumption is based on the relatively short charging times ($\leq$ 40 s) used in the PDP technique. The expression for the rate of trapping postulated by McNabb and Foster[5] to be $k'N(1 - n)c$ is consistent with equation (2) if it is assumed that $(1 - n)$ is constant on the time scale of the potential-step experiments. The trapping rate constant is then given by $k = k'N(1 - n)$.

Furthermore, the reversible traps are assumed to release all their hydrogen within the time of the anodic transient, t_a, so that all the hydrogen remaining in the metal at the end of t_a can be attributed to truly irreversible trapping. In the case of 4340 steel, this assumption is justified on the basis of the value of K_r, which is estimated to be 500 (discussed later). The reversible traps in 4340 steel[6] are typically in the range 10^{19}-10^{27} m^{-3}. Even using the lower limit of this range, k_r/p is 5 x 10^{-17} m^3, which implies that the release constant is large; therefore, the release rate will be rapid even when the fraction of traps occupied is very low. For the two nickel-based alloys, the binding energy for hydrogen to defects such as vacancies or edge dislocations in an fcc lattice is about 0.1

eV compared with roughly 0.4 eV for the activation energy for diffusion in this type of lattice.[7] Therefore, transport of hydrogen in such cases is limited by diffusion with little hindrance from reversible traps.

The diffusion equation (2) has been solved analytically[1] for two cases that are characterized by the rate-determining step for the transfer of H_{ads} into the metal during the charging time. In both cases, it is assumed that that the layer of H_{ads} adjusts very rapidly to a potential step. For a given value of the charging potential, E_c, the hydrogen ingress flux into the metal is considered to be constant. If the rate of transfer of hydrogen into and out of the metal is rapid, the concentration of hydrogen in the metal at $x = 0$ will be in equilibrium with the adsorbed hydrogen layer. The ingress of hydrogen is then under diffusion control in the bulk metal.

Conversely, if the rate of transfer of hydrogen atoms across the interface is slow, this rate will control the rate of ingress. At long enough times, the concentration immediately below the surface will approach the equilibrium value and a transition to diffusion control will then occur.

MATERIALS

AISI 4340 Steel

The 4340 steel was supplied as 1.27-cm plate produced from an argon-oxygen-decarburized heat and subsequently vacuum-arc remelted followed by forging, rolling, and annealing. The as-received plate was machined into two rods (1.25 cm in diameter and 5 cm long), which were heat treated to HRC values of 41 and 53, corresponding to yield strengths of 175 and 260 ksi, respectively.

The chemical composition of the alloy was provided by the manufacturer and is given in Table 1. The nature and distribution of inclusions were determined in an earlier study[8] and it was found that there were ~10^5 m^{-2} MnS inclusions randomly distributed through the material. The inclusions were ellipsoidal with the major axis transverse to the rolling direction. Based on a spherical shape for the inclusions, the density of inclusions was calculated to be 2 x 10^9 m^{-3} and the mean radius of the inclusions averaged over the transverse and parallel directions was 9.2 μm.

Monel K500

This alloy was supplied by Huntington Alloys as a 1.27-cm cold-drawn rod in an unaged condition. The HRC value of the as-received material was 26, which corresponds to a yield strength of ~110 ksi. A section of the rod was age-hardened to HRC 35, giving a yield strength of about 159 ksi. The chemical composition of the alloy is given in Table 1.

MP35N

MP35N is a vacuum-induction, vacuum-arc remelted alloy and was supplied by Latrobe Steel Co. as a 1.36-cm rod cold-drawn and aged. The hardness and yield strength for the as-received material were HRC 45 and 269 ksi, respectively. The composition provided by the manufacturer for the rod is given in Table 1.

Table 1

CHEMICAL COMPOSITION OF THE THREE ALLOYS TESTED

(wt%)

Element	4340	K500	MP35N
Fe	Bal	0.64	0.34
C	0.42	0.16	0.003
Mn	0.46	0.72	<0.01
P	0.009	n	0.003
S	0.001	0.001	0.002
Si	0.28	0.15	0.02
Cu	0.19	29.99	n
Ni	1.74	64.96	35.88
Cr	0.89	n	20.19
Mo	0.21	n	9.55
Al	0.031	2.92	n
N	0.005	n	n
O	0.001	n	n
Ti	n	0.46	0.85
Co	n	n	Bal

n = not present or not given.

EXPERIMENTAL PROCEDURE

Electrodes

The test electrodes of each alloy were fabricated from 5-cm lengths of rod. Each rod was press-fitted into a Teflon sheath so that only the planar end surface of the rod was exposed to the electrolyte. The surface was polished with successively finer grades of SiC paper from 320 to 600 grit followed by 0.05-μm alumina powder.

Cell

A conventional three-electrode electrochemical cell was used. The counter electrode was a graphite rod and the reference electrode assembly consisted of a saturated calomel electrode (SCE) inserted in a Luggin probe that was positioned 1-2 mm from the test electrode surface. All potentials are given with respect to the SCE. The electrolyte was an acetate buffer (1 mol L^{-1} acetic acid/ 1 mol L^{-1} sodium acetate, pH 4.8) containing 15 ppm As_2O_3 as a hydrogen entry promoter. Before the measurements began, the electrolyte was deaerated with argon for 1 hour. Argon purging was continued throughout data acquisition to promote mass transport of H^+ to the test electrode. All measurements were performed at 22 ± 2°C.

Instrumentation

The PDP technique was performed using a Princeton Applied Research Model 173 Potentiostat with a Model 276 Interface coupled to a Macintosh microcomputer via an Iotech Mac 488 Bus Controller. A BASIC program was developed to provide the perturbation (double-pulse) waveform, set control parameters, and perform data acquisition. The open-circuit potential, E_{oc}, of

the test electrode is sampled, and the electrode is then potentiostatically controlled at E_A, which is set to 10 mV negative of E_{oc}.

Control Parameters

The principal control parameters were the charging potential, E_c; the period of the anodic and cathodic transients, t_a and t_c, respectively; and the current sampling rate. The primary concern was to generate a sufficiently rapid discharge of H^+ during t_c to transfer a significant quantity of hydrogen into the metal, but avoid bubble formation on the surface.

The times of the cathodic charging were selected to be from 0.5 to 40 s. At times under 0.5 s, insufficient hydrogen enters the metal and also the current at very short times is dominated by charging of the double layer at the surface. In contrast, prolonged charging of the metal may result in saturation of traps, specifically those of the irreversible type, thereby invalidating the mathematical model used in the analysis. Moreover, at excessively long charging times, internal damage to the metal may occur due to the accumulation of hydrogen. The reproducibility of data for the charge passed during the anodic transient for consecutive tests with t_c = 40 s suggested that neither trap saturation or trap generation due to structural damage occurred. Furthermore, this upper limit provided a range of charging times covering almost two decades.

The time of data acquistion during the anodic transient was selected to be equal to that for the cathodic transient on the basis that this would allow enough time for the deepest untrapped hydrogen to diffuse back to the metal surface and also for hydrogen in highly reversible traps to be released, as discussed above.

The open-circuit potential was sampled before <u>each</u> charging time t_c and this new value used to set E_A. This approach allows for any drift in E_{oc} and

is therefore considered to accurately reflect the freely corroding condition of the metal at all times during the range of E_c and t_c values used. The practical consequence of this procedure is that it maintains E_A slightly negative of the existing E_{oc}, thereby minimizing anodic oxidation of the metal.

RESULTS

Method of Analysis

The anodic current transients characteristically exhibited the same shape over the range of charging potentials and times of interest for all the alloys. A typical transient is shown in Figure 1. It was found that the diffusion-control model was not valid for any of the three alloys, whereas the data in all cases could be analyzed in terms of the flux-control model. The total charge passed out is given in nondimensional form by

$$Q(\infty) = \sqrt{R}\{1 - e^{-R}/\sqrt{(\pi R)} - [1 - 1/(2R)]\mathrm{erf}\sqrt{R}\} \quad (6)$$

where the nondimensional terms are defined by $Q = q/[FJ\sqrt{(t_c/k)}]$ and $R = kt_c$. For the model to be applicable, it must be possible to determine a trapping constant for which the flux is constant over the range of charging times.

The analysis of data using the flux-control model was restricted to charging times from 10 to 40 s for two reasons: (1) At short charging times, the values of q_a may be significantly influenced by the contribution due to oxidation of the adsorbed hydrogen layer. It is assumed that q_a is associated entirely with oxidation of hydrogen that entered the metal. (2) The cathodic current during t_c decays to some extent in its early stages, which may affect the flux of hydrogen across the metal surface. The mass transport of H^+ to the metal surface during t_c is assumed to be constant; therefore, for those values of t_c (> 10 s) where the current is approximately constant for <u>most</u> of the charging time, this assumption is more justified.

4340 Steel

The data were analyzed in terms of the flux-control model and values of

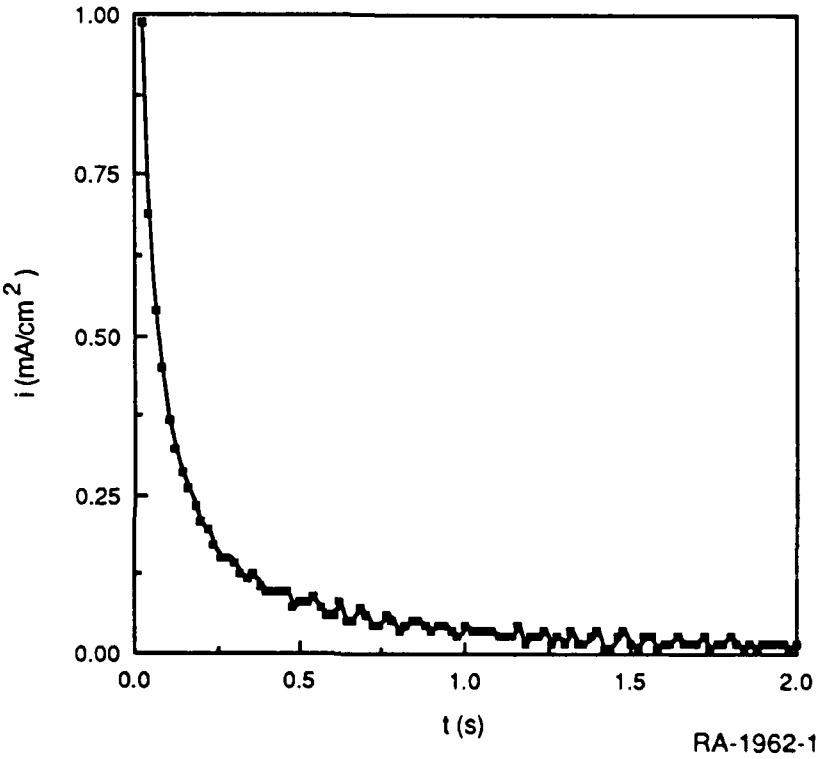

FIGURE 1 ANODIC TRANSIENT FOR 4340 STEEL HRC 53 CHARGED AT 10 s AND -0.985 V (SCE). Full transient is not shown.

the interfacial flux and trapping constant determined for charging times from 10 to 40 s are given for each potential step, $\eta\,(E_c - E_{oc})$, in Table 2.

Table 2

INTERFACIAL FLUX AND TRAPPING CONSTANTS FOR 4340 STEEL

Type	η (V)	J (nmol cm^{-2} s^{-1})	k_a (s^{-1})
HRC 41	-0.35	0.07	0.0058
	-0.40	0.19	0.008
	-0.45	0.36	0.008
HRC 53	-0.35	0.13	0.0066
	-0.40	0.26	0.008
	-0.45	0.55	0.009

For both heat-treated specimens, k_a is essentially independent of η, as expected because the density of traps within the metal should not be affected by the electrochemical surface conditions. Moreover, in both cases, k_a has approximately the same value of 0.008 s^{-1}. Using this value and the appropriate value of J in equation (6), q_a was calculated for charging times from 0.5 to 40 s and compared with the corresponding experimental results. The two sets of data for HRC 53 and η = -0.4 V are shown in Figure 2, where Q' is given by $Q'(\infty)V(t_c/k) = q_a/FJ$. The form of the curves and the close fit between them are typical for both specimens. The agreement between the two sets of data indicates the independence of both k and J with respect to t_c. However, the flux does increase with η, which is due to the dependence of J on the surface coverage of H_{ads} and therefore on potential. The surface coverage and therefore the flux should exhibit an exponential dependence on potential, which is in fact observed for both specimens, as shown in logarithmic form in

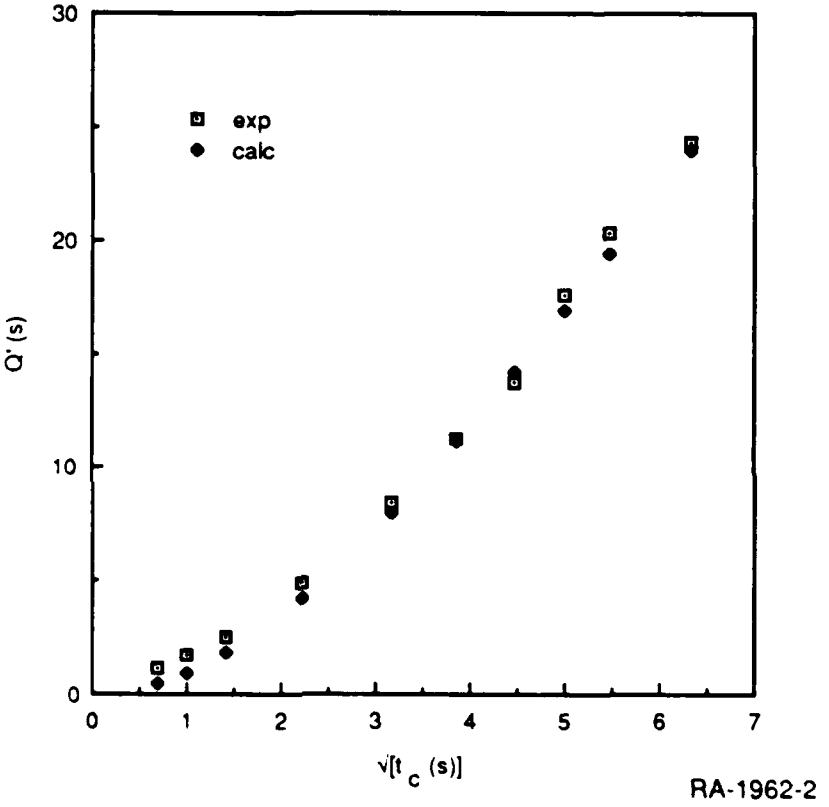

FIGURE 2 COMPARISON OF CHARGE DATA FOR 4340 STEEL HRC 53 CHARGED AT -0.985 V (SCE).

Figure 3. Interestingly, although the amount of data is limited, the two slopes (-7.1 and -6.3) appear to be close, suggesting that the rate constant for the flux across the interface is determined primarily by electrochemical characteristics and not by alloy microstructure.

Monel K500

Values of the interfacial flux and trapping constant determined for charging times from 10 to 40 s are given in Table 3. At more negative overpotentials, E_{oc} shifts sharply to more negative values during the range of charging times used and extensive bubble formation occurs. The shift in E_{oc} probably reflects reduction of an oxide film on the alloy surface, implying that at lower values of η, the reduction of H^+ and the subsequent entry of H atoms into the metal occurred on an oxide-covered surface. This would account for the large overpotentials required to achieve a significant ingress of hydrogen into the metal compared with those for the steel.

Table 3

INTERFACIAL FLUX AND TRAPPING CONSTANTS FOR MONEL K500

Type	η (V)	J (nmol cm^{-2} s^{-1})	k_a (s^{-1})
AR	-0.70	0.18	0.027
	-0.80	0.21	0.027
HRC 35	-0.65	0.12	0.016
	-0.70	0.17	0.016
	-0.75	0.17	0.012

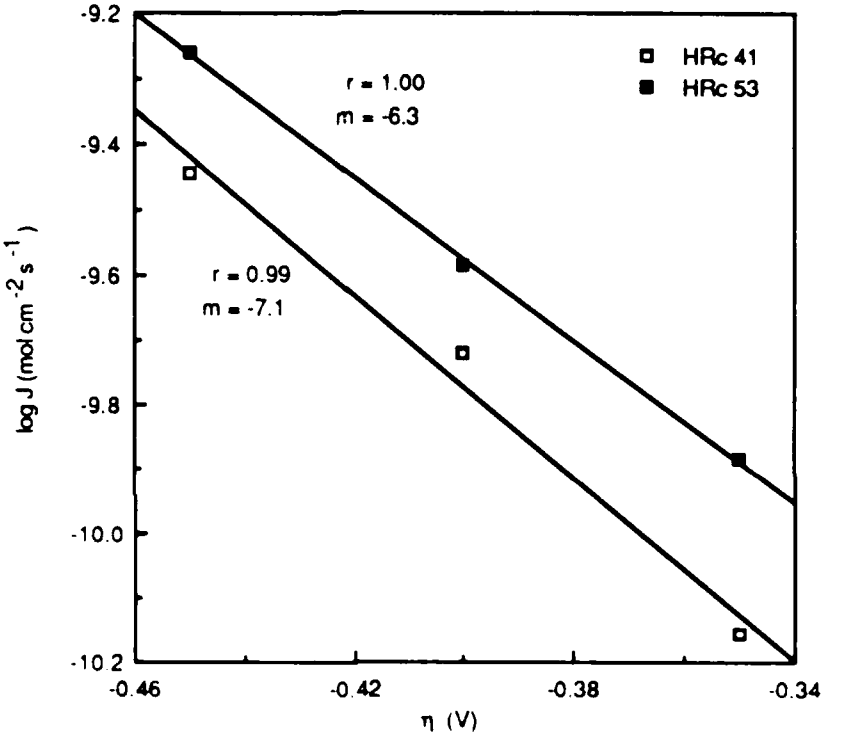

FIGURE 3 DEPENDENCE OF FLUX ON OVERPOTENTIAL

For both Monel specimens, the results exhibit similar patterns to those for 4340 steel: (1) k_a is essentially independent of E_c although, unlike 4340 steel, k_a differs for the two specimens. This decrease with aging can be attributed to either an increase in K_r for a given k or a decrease in the number of irreversible traps and therefore k. (2) The flux increases with η, but not to the same extent as it does for 4340 steel.

MP35N

The behavior of this alloy was similar to but more marked than that of the Monel. The presence of a film was indicated by a significant negative shift in E_{oc} during the range of charging times at η = -0.55 V and also a dramatic increase in the values of q_a for this potential compared with those at lower potentials. Evidently, H ingress, as with Monel, occurs across a surface film.

Values of J and k_a determined for charging times from 10 to 40 s are given in Table 4. The value of k_a is constant for the two lower values of η, but decreases as E_c becomes more negative. This decrease is regarded as an artifact resulting from partial film reduction/repassivation, which inflates the value of q_a, making it appear that less hydrogen was trapped in the metal during egress and therefore resulting in an apparent decrease in k. Accordingly, a value of 0.025 is considered to be reliable for k_a in the case of MP35N.

Table 4

INTERFACIAL FLUX AND TRAPPING CONSTANTS FOR MP35N

η (V)	J (nmol cm^{-2} s^{-1})	k_a (s^{-1})
-0.40	0.05	0.024
-0.45	0.08	0.026
-0.50	0.08	0.004
-0.55	0.19	0.0002

DISCUSSION

4340 Steel

The irreversible trapping constant, k, for 4340 steel can be obtained from the value of k_a using diffusivity data. The value of D_a for hydrogen in HRC 50 electroslag remelted (ESR) 4340 was found from membrane permeation experiments[9] to be ~10^{-7} cm^2 s^{-1}. The difference in diffusivity between this ESR steel and the VAR-produced specimen used in this study is assumed to be small enough to ignore; that is, it should be at least within the same order of magnitude. Data reported for D_L in pure iron show a considerable variation, but a value of about 5 x 10^{-5} cm^2 s^{-1} at 25°C appears to be reliable.[10,11] Using these values for D_a and D_L in equation (4), K_r is found to be approximately 500, and therefore the value of k from equation (3) is 4 s^{-1}.

The trapping constant can be regarded as the mean trapping frequency of a single hydrogen atom in the metal lattice and can be related to the trap density on the basis of several simple models.[2] One such model for interpreting the magnitude of k is based on the assumption of spherical traps of surface area $4\pi d^2$. This model yields the following expression for k in terms of the concentration, N_T, of traps:

$$k = 4\pi d^2 N_T D_L / a \qquad (6)$$

The diameter, a, of the iron atom is 248 pm but a value for d is also required to estimate N_T. This in turn presupposes a prior knowledge of potential irreversible traps. In the case of 4340 steel, these are likely to be MnS inclusions which are known[12] to be strong traps. The ellipsoidal shape of the MnS inclusions in the test specimen means that the assumption of spherical traps in the above model is somewhat of an approximation. However, using the value of 9.2 μm for the mean radius of the MnS inclusions, the density of

traps is found to be 2 x 10^8 m^{-3}. In view of the assumed spherical shape for the traps and also the MnS inclusions, this value is in reasonable agreement with the actual number of inclusions, 2 x 10^9 m^{-3}. Moreover, the value of N_T is the same for both the HRC 41 and 53 specimens, which further indicates that the irreversible traps determined from the PDP measurements are MnS inclusions because their content should not be altered by heat treatment.

The participation of other irreversible traps such as Fe_3C and TiC interfaces is possible, but it seems that they can have only a relatively minor role based on the value of N_T. Although the calculated trap density was obtained using the mean radius of the MnS inclusions, to achieve a value of N_T that approached the typical levels of Fe_3C and TiC interfaces in steels (10^{24}-10^{25} m^{-3}),[6] an unreasonably small value of 0.01-0.1 pm (3-4 orders of magnitude smaller than the radius of the iron atom) for d would be required for k = 4 s^{-1}.

Monel K500

Evaluation of the irreversible trapping constant, k, from the value of k_a requires diffusivity data for the appropriate Cu/Ni alloy and also Monel K500. The diffusivity of hydrogen in 30 at.% Cu-70 at.% Ni is 3 x 10^{-10} cm^2 s^{-1} at 25°C,[13] but it apparently has not been reported for Monel K500. However, the relatively large activation energy for H diffusion in an fcc lattice compared with the binding energy at typically reversible traps suggests that trapping at such sites is only a small perturbation on H diffusion. Therefore, in view of the low diffusivity in the Cu/Ni alloy, the presence of other elements in an fcc lattice, specifically those acting as reversible traps, should have little effect on D_L compared with the effect in iron where the true lattice diffusivity is 5 orders of magnitude higher. On this basis, $D_a \approx D_L$, and therefore, it will be assumed that $k \approx k_a$. However, the rate constant approximation is liable to considerable inaccuracy because, although K_r may have little effect relative to the low diffusivity of the Cu/Ni alloy, it may

cause a relatively significant change to k_a.

Hydrogen embrittlement in Cu-Ni base alloys is known to be assisted by segregated sulfur.[14] If the primary irreversible trap in both Monel specimens is assumed to be S (considered in the atomic form rather than as a copper-nickel sulfide), then d can be taken as the atomic radius of S. The value of a is determined from the weighted mean atomic diameter of Cu (256 pm) and Ni (250 pm). Therefore, using d = 104 pm, a = 252 pm, $D_L = 3 \times 10^{-10}$ cm^2 s^{-1}, and k = 0.027 s^{-1}, the density of irreversible traps HRC 26 Monel is found to be 1.7×10^{21} m^{-3}. The corresponding density in the HRC 35 specimen (k = 0.016 s^{-1}) is 9.9×10^{20} m^{-3}. The actual number of S atoms can be calculated from the density of Monel K500 (8.43 g cm^{-3}) and the wt% data for S in Table 1, and is found to be 1.6×10^{24} S atoms/m^3 for the AR Monel. This figure is assumed to apply also to the aged Monel although the distribution of S will probably be different due to segregation at grain boundaries.

The difference of 3-4 orders of magnitude between the value of N_T and the number of S atoms may indicate that these elements are not the primary irreversible traps. However, the two figures can be reconciled to a large extent in terms of irreversible S traps on the basis of the diffusivity, D_L, and the presence of reversible traps. Although the effect of reversible traps on k was neglected, this is undoubtedly a gross approximation, and it is possible that K_r is of the order of 10 or higher, which would increase k and therefore N_T. Furthermore, it is debatable how accurately the diffusivity for the Cu-Ni alloy can be applied to the Monel, which differs to a small extent in the levels of Cu and Ni and does not reflect the presence of minor alloying elements, particularly since the effect of these elements was not taken into account in the K_r term for the trapping constants.

MP35N

Evaluation of k from the value of k_a requires diffusivity data for the "pure" Co-Ni-Cr-Mo alloy and also MP35N. However, the most appropriate data for the pure alloy pertains to 50 at.% Co-50 at.% Ni for which D_L is 5.5 x 10^{-11} cm^2 s^{-1} at 25°C.[13] The effect of the other two primary and also the minor alloying elements in MP35N may result in a considerable difference in diffusivity between the Co-Ni alloy and the quaternary base of MP35N. Nevertheless, in the absence of diffusivity data for MP35N, it is assumed that, like the Monel, other elements, particularly those acting as reversible traps, will have little effect on the low diffusivity in the Co/Ni fcc lattice. On this basis, $D_a \approx D_L$, and therefore it is also assumed that $k \approx k_a$

The resistance of MP35N to hydrogen embrittlement has been correlated with the concentration of P and S impurities on the major crystallographic boundaries.[15] If the S and P (in atomic form) are treated as the primary irreversible traps, d can be taken as the mean atomic radius of S (104 pm) and P (110 pm). Likewise, the value used for a is the mean diameter of Co (250 pm) and Ni (250 pm). Therefore, using d = 107 pm, a = 250 pm, D_L = 5.5 x 10^{-11} cm^2 s^{-1}, and k = 0.025 s^{-1}, N_T is found to be 7.9 x 10^{21} m^{-3}.

The actual number of S and P atoms calculated from the density of MP35N (8.43 g cm^{-3}) and the wt% data for these elements in Table 1 is 8.1 x 10^{24} S and P atoms m^{-3}. The difference of three orders of magnitude between the value of N_T and the density of S and P atoms, as with the Monel, may indicate that these elements are not the primary irreversible traps. Nevertheless, the two figures can largely be reconciled in terms of similar considerations to those for the Monel.

Of particular significance is a lower value of D_L and therefore an increase in N_T. The value of D_L for the 50 at.% Co-50 at.% Ni alloy may well differ appreciably for a Co-Ni-Cr-Mo alloy. The diffusivity for 46 at.% Cu-54

at.% Ni[13] is 1.8×10^{-10} cm^2 s^{-1}, so the change from Cu to Co decreases D_L by a factor of 2, and larger decreases are likely with the addition of Cr and Mo. For example, the addition of 20 at.% Cr to Fe at 27°C decreases D_L by three orders of magnitude[16] although the effect for the bcc lattice would be more pronounced than that for an fcc lattice. Therefore, in view of the lack of appropriate diffusivity data for the "pure" quaternary alloy as well as the approximation regarding the value of k, it is still possible that the S and P impurities are in fact the principal irreversible traps in MP35N.

SUMMARY

Hydrogen ingress in all three high-strength alloys, 4340 steel, Monel K500, and MP35N, occurs under interfacial control whereby the rate of ingress is determined by the flux across the alloy surface into the bulk and not by H diffusion in the alloy.

The rate constant for irreversible trapping in 4340 steel was determined from the measured rate constant by estimating the effect of reversible traps from diffusivity data. The value of k was found to be 4 s^{-1} for both HRC 41 and 53 specimens, and the density of traps derived from k, 2 x 10^{8} m^{-3}, indicated that the primary reversible traps were MnS inclusions, which was supported by the fact that the same value of k and therefore trap density was obtained for both heat-treated specimens.

The irreversible trapping constant for Monel K500 was approximated to the apparent trapping constant, thereby yielding a density of traps that was 3-4 orders of magnitude less than the number of S atoms, which is probably within the accuracy of the approximations for the available data.

The density of traps for MP35N, like Monel, can be evaluated only by approximating k to the apparent trapping constant and similarly is three orders of magnitude less than the number of S and P impurities. This difference can be explained by factors similar to those for Monel, that is, applicability of available data.

ACKNOWLEDGEMENTS

The author gratefully acknowledges the assistance of Dr. L. Eiselstein of SRI's Poulter Laboratory in providing the 4340 steel plate, heat-treating the 4340 specimens and measuring their hardness.

REFERENCES

1. R. McKibbin, D. A. Harrington, B. G. Pound, R. M. Sharp, and G. A. Wright, Acta Met. **35**, 253 (1987).

2. B. G. Pound, R. M. Sharp, and G. A. Wright, Acta Met. **35**, 263 (1987).

3. J. O'M. Bockris, M. A. Genshaw, and M. Fullenwider, Electrochim. Acta **15**, 47 (1970).

4. I. M. Bernstein and A. W. Thompson, in Advanced Techniques for Characterizing Hydrogen in Metals, N. F. Fiore and B. J. Berkowitz, Eds., Proc. Sym. AIME, Kentucky (1981), p. 89.

5. A. McNabb and P. K. Foster, Trans. Met. Soc. AIME **227**, 618 (1963).

6. R. Gibala and D. S. DeMiglio, in Proc. 3rd Int. Conf. on Effect of Hydrogen on Behavior of Materials, I. M. Bernstein and A. W. Thompson, Eds., The Metallurgical Soc. of AIME, Moran, Wyoming (1980), p.113.

7. W. D. Wilson and S. C. Keeton, in Advanced Techniques for Characterizing Hydrogen in Metals, N. F. Fiore and B. J. Berkowitz, Eds., Proc. Sym. AIME, Kentucky (1981), p.3.

8. D. A. Shockey, D. R. Curran, and L. Seaman, "Development of Improved Dynamic Failure Models," SRI International, Final Report to U.S. Army Research Office, Contract No. DAAG-29-81-K-0123 (1985).

9. J. A. Kargol and L. D. Paul, in Proc. 1st Int. Conf. on Current Solutions to Hydrogen Problems in Steels, C. G. Interrante and G. M. Pressouyre, Eds., ASM, Washington, DC (1982), p.91.

10. R. A. Oriani, Acta Met. **18**, 147 (1970).

11. A. J. Kumnick and H. H. Johnson, Met. Trans. **5**, 1199 (1974).

12. J. Y. Lee, J. L. Lee, and W. Y. Choo, in Proc. 1st Int. Conf. on Current Solutions to Hydrogen Problems in Steels, C. G. Interrante and G. M. Pressouyre, Eds., ASM, Washington, DC (1982), p.423.

13. H. Hagi, Trans Jap. Inst. Metals, **27**, 233 (1986).

14. J. D. Frandsen and H. L. Marcus, "Crack Growth and Fracture in Gaseous Hydrogen", in Effect of Hydrogen in Behavior of Materials, A. W. Thompson and I. M. Bernstein, Eds., TMS-AIME, (1976), p.233.

16. R. D. Kane and B. J. Berkowitz, Corrosion **36**, 29 (1980).

17. J. O'M. Bockris, M. A. Genshaw and M. Fullenwider, Electrochim. Acta **15**, 47 (1970).

END

7-87

DTIC